

# High-Temperature Spectral Emissivity of Several Refractory Elements and Alloys

R.N. Wall, D.R. Basch, and D.L. Jacobson

Thermionic energy conversion has emerged as the method of choice for the direct space-based conversion of heat to electricity. An important parameter in the implementation of this method of direct energy conversion is the emissivity of the converter emitter and collector materials. This information is necessary to determine heat losses, heat transfer, and reservoir temperatures in the thermionic energy converter. Spectral normal emissivities were acquired at a wavelength of 0.65  $\mu\text{m}$  for a series of tungsten-rhenium alloys, tungsten-osmium alloys, and tungsten-iridium alloys in the temperature range 1400 to 2600 K. Additionally, the spectral normal emissivity for pure elements of molybdenum and ruthenium were obtained over the temperature range 1200 to 2600 K and 1400 to 2250 K, respectively. The spectral normal emissivities for a niobium-67% ruthenium (eutectic composition) in the temperature range 1400 to 2000 K were also obtained at the same wavelength. In all cases, the emissivity decreased linearly with increasing temperature. Both the tungsten-osmium and the tungsten-rhenium alloys exhibited emissivity values of 0.32 to 0.54 over the temperatures tested. The tungsten-iridium alloy yielded emissivity data of 0.35 to 0.47. The niobium-ruthenium emissivity data were within 0.34 and 0.36. The pure molybdenum and pure ruthenium experiments resulted in emissivity values ranging from 0.35 to 0.45 and 0.35 to 0.39, respectively.

## 1. Introduction

THE use of thermionic energy conversion (TEC) to generate the gigawatt to megawatt power levels needed to energize various electrical components in extraterrestrial environments has proven highly desirable. The thermionic energy converter provides the capability to convert heat directly to electricity without the complications introduced by moving system components. This method also facilitates the generation of energy with high heat rejection temperatures, an important asset when minimization of launch weight is critical.

There are many important material parameters that must be investigated during the design and fabrication of practical thermionic converters. However, emitter and collector materials properties constitute the most important of these variables. Such material characteristics include the high-temperature mechanical properties, corrosion resistance in a cesiated environment, effective work function, and thermal radiative properties. Radiative properties have been shown to be very sensitive to methods of preparation, thermal history, and environmental conditions.<sup>[1]</sup> Also, the importance of surface films and composition<sup>[2]</sup> cannot be ignored. Such effects are most significant at high temperatures,<sup>[3]</sup> where the reaction rates are greatest.

Because emissivity is generally a strong function of the surface roughness, particular attention was given to surface preparation and characterization. Each sample was ground using a diamond-impregnated grinding wheel ( $R_q = 8$  to 15 rms surface roughness).

Surface roughness analysis was accomplished using a Taylor-Hobson Talysurf 10 profilometer. The emissivities were

calculated by comparing the surface brightness temperature and the temperature obtained from an adjacent hohlraum (*i.e.*, a cylindrical hole approximating a black body) with a depth-to-diameter ratio of at least ten. Both the surface brightness temperature and the hohlraum temperature were obtained using a micro-optical disappearing filament pyrometer. The objective in this series of experiments was to obtain the spectral normal emissivities for several series of tungsten-base alloys as a function of time, temperature, and alloy composition.

## 2. Sample Fabrication and Preparation

It is known that the emissivity of many materials exhibits a strong surface texture dependence.<sup>[4]</sup> Therefore, surface preparation was accomplished in a precise manner. Surfaces were ground using a DoAll diamond-impregnated grinding wheel ( $R_q = 8$  to 15 rms surface roughness). The surface textures were characterized<sup>[5]</sup> using a Taylor-Hobson Talysurf 10. The results of these measurements are reported in Table 1.

Each sample was 9.2 mm in diameter and approximately 2.0 mm thick. Hohlräume (*i.e.*, a cylindrical hole approximating a black body) with depth-to-diameter ratios of at least ten<sup>[6]</sup> were machined by electrical discharge machining (EDM). The surfaces surrounding the hohlräume were used to measure surface brightness temperature.

### 2.1. Tungsten-Rhenium Alloys

Four tungsten-rhenium samples were machined from sintered tungsten-rhenium rods. The rods were obtained from Arizona State University Thermionic Laboratory stock and were of unknown chemical composition. By averaging wavelength dispersive X-ray analysis (WDX) and electron microprobe (EMP) results and rounding to the nearest whole number, the four samples were designated W-3Re, W-10Re, W-24Re, and W-27Re. The accuracy was estimated  $\pm 3$  wt. % Re.

Ralph N. Wall, Advanced Semiconductor Technology Center, IBM East Fishkill Facility, Hopewell Junction, New York; and David R. Basch and Dean L. Jacobson, Arizona State University, Department of Chemical, Bio, and Materials Engineering, Tempe, Arizona.

## 2.2. Tungsten-Osmium Alloys

Three tungsten-osmium alloys provided by Dr. Edmund K. Storms (Los Alamos Scientific Laboratory) were prepared by mixing and pressing the pure powder followed by subsequent sintering at high temperature. The sintered material was then repeatedly arc melted. A fourth alloy was prepared in like fashion, but was not subjected to arc melting.

Sample compositions were determined by weighing the powders before mixing and verifying with WDX analysis. The samples were designated W-5Os, W-9Os, and W-13Os for the arc-melted alloys and sintered W-5Os for the sintered alloy. The compositions were deemed accurate to  $\pm 1$  wt.% Os.

## 2.3. Tungsten-Iridium Alloys

Four tungsten-iridium alloys provided by Dr. Storms were prepared by mixing small chunks of high-purity iridium with tungsten powder. Sintered pellets were formed and subsequently subjected to repeated arc melting. Before mixing, the metals were weighed, thus allowing accurate calculation of the composition. The compositions were rounded to the nearest whole number and then designated W-1Ir, W-3Ir, W-5Ir, and W-7Ir. A fifth sample, also prepared by arc melting, was furnished by Ames Laboratories (Iowa State University) and had a reported content of 0.3 wt.% Ir. This sample was designated W-0.3Ir. Chemical compositions were estimated to be accurate to less than  $\pm 1$  wt.% Ir.

## 2.4. Niobium-Ruthenium Alloy and Pure Metals

A sintered rod of eutectic composition niobium-ruthenium (Nb-67Ru) was purchased from Materials Research Corp. (Orangeburg, New York). A high-purity (99.97%) molybdenum rod and a polycrystalline sample of ruthenium were purchased from Alfa Products (Dunrers, Massachusetts).

## 3. Experimental Procedure

The vacuum spectral normal emissivity was calculated from the measured black body hohlraum temperature and surface brightness temperature measurements. Data were acquired by a micro-optical disappearing filament pyrometer through a calibrated sapphire high-vacuum viewport. The micro-optical disappearing filament pyrometer was calibrated using a National Institute of Standards and Technology tungsten strip lamp. The viewport was protected from condensing vapors by a stainless steel shutter. A vacuum of  $10^{-9}$  to  $10^{-7}$  torr was maintained using a large ion sputter pump. Figure 1 illustrates the high-temperature sample holder configuration.

The spectral normal emissivity is defined as the ratio of energy at a particular wavelength,  $\lambda$ , emitted in the normal direction from the surface of a material, to the energy emitted at that same wavelength from a black body operated at the same temperature. Mathematically:

$$\epsilon_{\lambda} = \frac{W_{\lambda}}{W_{\lambda b}} \quad [1]$$

where  $\epsilon_{\lambda}$  is the spectral normal emissivity at wavelength  $\lambda$ ,  $W_{\lambda}$  is the radiation energy normal to the surface, and  $W_{\lambda b}$  is the radiation energy normal to a black body. Both  $W_{\lambda}$  and  $W_{\lambda b}$  must be measured at the same temperature.

In most cases, the spectral normal emissivity of a material is a function of both temperature and the wavelength at which it is measured. In this work, emissivity was determined as a function of time and temperature at a wavelength of  $0.65 \mu\text{m}$ . All other wavelengths were filtered. By applying Planck's law<sup>[7]</sup> and Wien's approximation,<sup>[8]</sup> Eq 1 may be written:<sup>[9]</sup>

$$\epsilon_{\lambda} = \exp \left[ \frac{C_2}{\lambda} \left( \frac{1}{T_B} - \frac{1}{T_S} \right) \right] \quad [2]$$

where  $C_2$  is Planck's second constant ( $14\,388 \mu\text{m}\cdot\text{K}$ ),  $T_B$  is the black body temperature, and  $T_S$  is the surface brightness temperature.  $T_S$  represents the measured temperature and should not be construed to suggest that the actual surface temperature is different from the bulk.  $T_B$  is the true temperature of the bulk and presumably of the surface.

## 4. Results and Discussion

### 4.1. Tungsten-Rhenium Alloys

The spectral normal emissivities, as a function of temperature, measured at a wavelength of  $0.65 \mu\text{m}$  for the tungsten-rhenium alloys tested in this work are summarized in Fig. 2. Figure 3 presents experimental data reported in the literature for pure samples of tungsten,<sup>[10,11]</sup> rhenium,<sup>[12,13]</sup> and os-

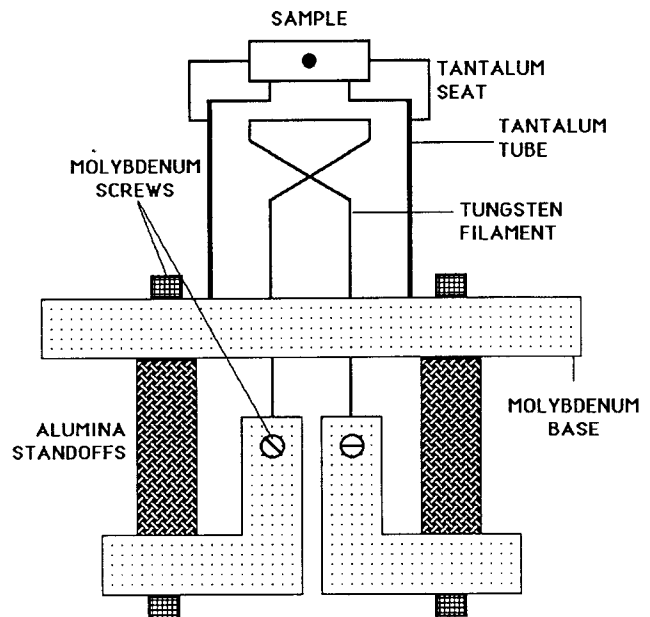


Fig. 1 High-temperature (up to 2900 K) sample holder used in the vacuum emission vehicle.<sup>[20]</sup>

mium<sup>[14]</sup> for comparative purposes. Linear equations representing emissivity as a function of temperature for these alloys are shown in Table 2. The alloys exhibited the lowest emissivity values at the highest percent alloy addition. Furthermore, for each system, a maximum emissivity was obtained for compositions approximately in the middle of the respective solid solution regions. There was no apparent correlation between the surface texture, summarized in Table 1, and the observed emissivities for these alloys. No significant time dependence with respect to emissivity was observed.

It is apparent that temperature measurements by optical pyrometry of a hot surface must be corrected using an appropriate emissivity value. Many tungsten alloy studies, for example, used a value of 0.42 to correct surface temperature without regard for the alloy composition or temperature (*e.g.*, Ref 15).

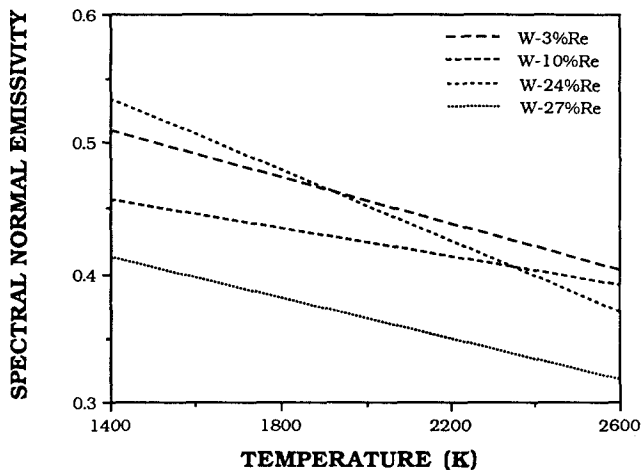


Fig. 2 Comparison of spectral normal emissivity at 0.65  $\mu\text{m}$  of tungsten-rhenium alloys.

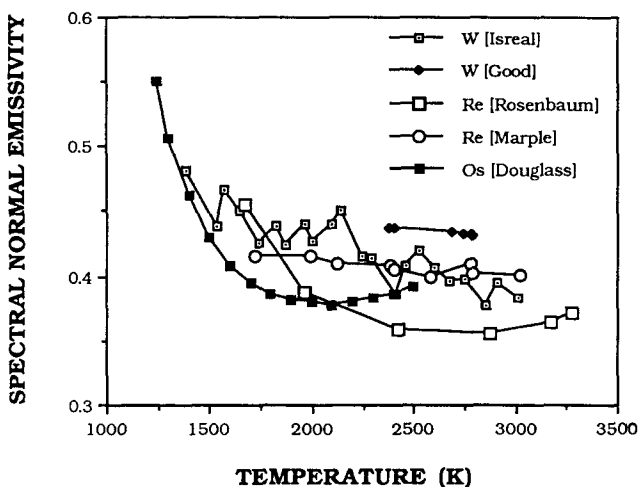


Fig. 3 Experimental data for pure tungsten, rhenium, and osmium at 0.65  $\mu\text{m}$ .

Significant error is introduced by following such a procedure. Moraga<sup>[16]</sup> reported spectral normal emissivities at 0.535  $\mu\text{m}$ , also measured in vacuum, for several tungsten-rhenium alloys. The data of Moraga's, for the most part, closely paralleled those of the current study.

The data used in plotting Fig. 2, 4, and 5 are represented by linear lines to remove confusion from the plot and still show all samples for a series of alloys on one plot. The relative uncertainty associated with the spectral normal emissivity calculations has been determined to be 2.5%. A detailed discussion of the uncertainty is given by Moraga.<sup>[16]</sup>

#### 4.2. Tungsten-Osmium Alloys

The spectral normal emissivity data for each tungsten-osmium composition were obtained and summarized in Fig. 4. Similar to the tungsten-rhenium case, the tungsten-osmium alloys exhibited the lowest emissivity values at the highest percent alloy addition. Furthermore, for each sample, a maximum emissivity was obtained for compositions in the middle of the solid solution region. Table 2 lists the linear equations for the emissivity as a function of temperature for each tungsten-os-

Table 1 Surface Texture Measurements

Sample	Surface roughness ( $R_a$ ), $\mu\text{in.}$	Sample	Surface roughness ( $R_a$ ), $\mu\text{in.}$
W-03Ir.....	...	W-3Re	46
W-11Ir.....	19	W-10Re	23
W-3Ir.....	14	W-24Re	39
W-5Ir.....	10	W-27Re	32
W-7Ir.....	10		
W-5Os.....	19	Nb-67Ru	10
W-9Os.....	8	Mo	12
W-13Os.....	12	Ru	...

Note: Use of ... indicates that sample was unavailable for characterization. Accuracy  $\pm 3\%$  of reading.

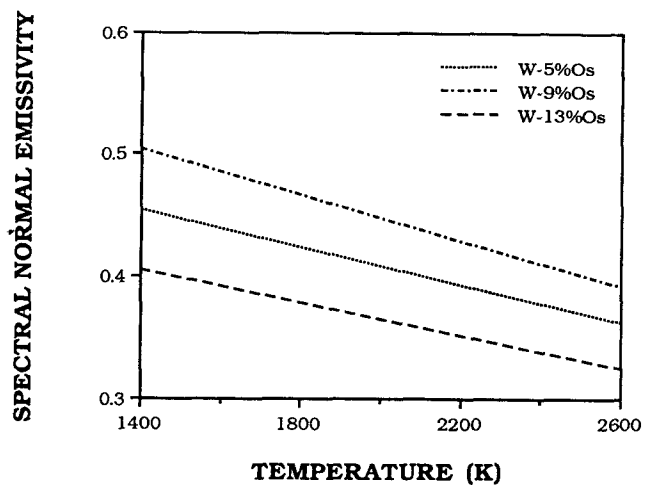


Fig. 4 Comparison of spectral normal emissivity at 0.65  $\mu\text{m}$  of tungsten-osmium alloys.

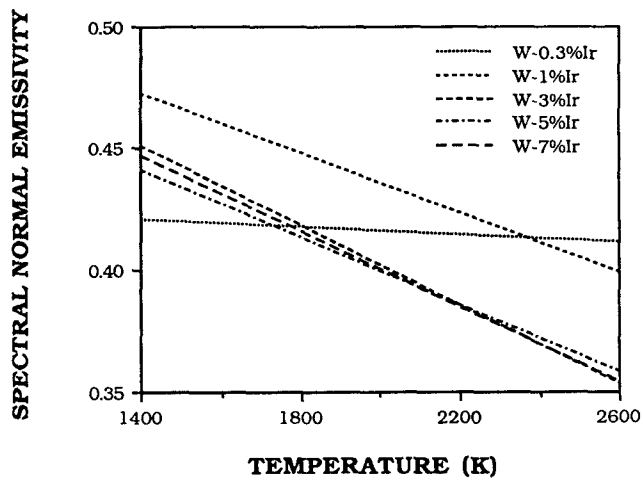


Fig. 5 Comparison of spectral normal emissivity at 0.65  $\mu\text{m}$  of tungsten-iridium alloys.

Table 2 Spectral Normal Emissivity of Tungsten-Base Alloys at 0.65  $\mu\text{m}$

Sample	Emissivity equation
W-3Re .....	$\epsilon_{0.65} = 0.635 - 8.954 \times 10^{-5} T$
W-10Re .....	$\epsilon_{0.65} = 0.534 - 5.525 \times 10^{-5} T$
W-24Re .....	$\epsilon_{0.65} = 0.727 - 1.373 \times 10^{-4} T$
W-27Re .....	$\epsilon_{0.65} = 0.525 - 7.994 \times 10^{-5} T$
W-5Os .....	$\epsilon_{0.65} = 0.561 - 7.624 \times 10^{-5} T$
W-9Os .....	$\epsilon_{0.65} = 0.632 - 9.240 \times 10^{-5} T$
W-13Os .....	$\epsilon_{0.65} = 0.499 - 6.699 \times 10^{-5} T$
W-0.3Ir .....	$\epsilon_{0.65} = 0.430 - 7.295 \times 10^{-6} T$
W-1Ir .....	$\epsilon_{0.65} = 0.558 - 6.114 \times 10^{-5} T$
W-3Ir .....	$\epsilon_{0.65} = 0.564 - 8.121 \times 10^{-5} T$
W-5Ir .....	$\epsilon_{0.65} = 0.538 - 6.899 \times 10^{-5} T$
W-7Ir .....	$\epsilon_{0.65} = 0.555 - 7.728 \times 10^{-5} T$
Ru .....	$\epsilon_{0.65} = 0.330 - 3.27 \times 10^{-5} T$
Mo .....	$\epsilon_{0.65} = 0.560 - 9.05 \times 10^{-5} T$

mium sample. Again, no significant correlation between surface texture and emissivity could be made. No significant time dependence with respect to emissivity was observed.

In earlier work,<sup>[17]</sup> it was shown that the surface composition for these W-Os alloys varied from the bulk composition (at these high temperatures). Also, the work function depended on the surface composition, not the bulk. Because the emissivity data did not follow the same trends as the work function data, and using knowledge of surface compositions, it was concluded that the bulk osmium concentration governs emissivity in this series of alloys.

#### 4.3. Tungsten-Iridium Alloys

Tungsten-iridium emissivities were measured and are compared in Fig. 5. The observed trends in the emissivity data were similar to the other tungsten alloys investigated in this work.

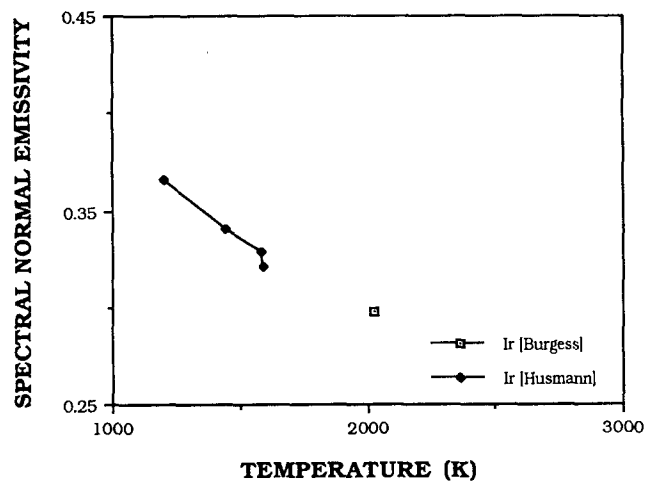


Fig. 6 Experimental data for pure iridium at 0.65  $\mu\text{m}$ .

The highest iridium concentrations produced the lowest emissivities. The measured emissivity data for W-0.3Ir were nearly identical to reported results for pure tungsten. W-1Ir yielded the highest emissivity of the tungsten-iridium compositions tested. Table 2 lists the straight line equations for the emissivity versus temperature data, and Fig. 6 presents experimental data reported in the literature<sup>[18,19]</sup> for pure iridium. Again, no significant time dependence with respect to emissivity was observed.

The similarity in the emissivities observed for W-3Ir, W-5Ir, and W-7Ir might be attributable to similar surface iridium concentrations (in contrast to W-Os). Similar trends were reported in work function for these alloys and were shown to be related to the surface composition.<sup>[20]</sup> Also, the trends exhibited in emissivity and work function for the W-0.3Ir and W-1Ir samples may be related to the depletion of iridium on the sample surface with increasing temperature (the W-0.3Ir work function was virtually identical to that of tungsten).

#### 4.4. Niobium-Ruthenium Alloy

The emissivity values, as a function of temperature, for eutectic niobium-ruthenium alloy (Nb-67Ru) are shown in Fig. 7, and the linear equation for these data are shown in Table 2. Figure 7 also presents experimental emissivity values reported in the literature for pure niobium<sup>[21]</sup> and pure ruthenium<sup>[22]</sup> for comparative purposes, respectively. As with the previous alloys, no significant time dependence with respect to emissivity was observed.

#### 4.5. Pure Metals

The emissivity data obtained for pure ruthenium is shown in Fig. 7, and the linear regression equation representing the data shown in Fig. 7 is listed in Table 2. The emissivity values, in this case, were largely constant, with only a slight decrease as a function of increasing temperature. No significant time dependence with respect to emissivity was observed.

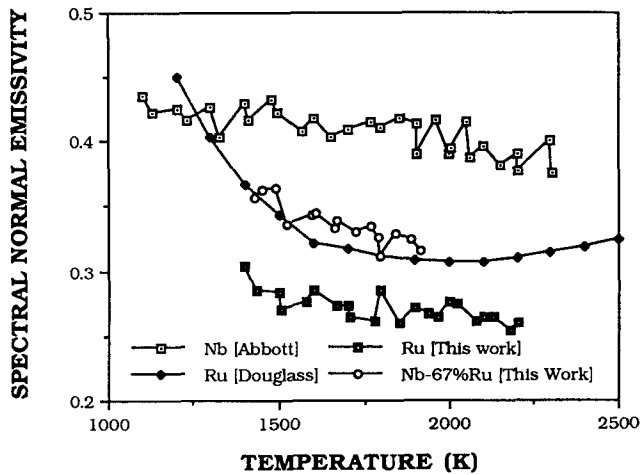


Fig. 7 Spectral normal emissivity of Nb-67Ru and pure niobium and pure ruthenium at 0.65  $\mu\text{m}$ .

The spectral normal emissivity data as a function of temperature for pure molybdenum are shown in Fig. 8 along with the results obtained by Baldwin<sup>[23]</sup> and Abbott.<sup>[24]</sup> The data obtained in the present work paralleled the data of Baldwin. Both sets of data demonstrate a slight decrease in emissivity with increasing temperature, whereas the data of Abbott were approximately constant.

## 5. Conclusions

The emissivity of an alloy is a strong function of alloy composition. The emissivity values for tungsten-base alloys exhibit a strong temperature dependence. Tungsten alloys with solid solution compositions in the midrange for the respective alloys exhibit greater emissivity values. Tungsten alloys in the two-phase region yield lower emissivity values. Surface composition of refractory alloys may have been significant with tungsten-iridium alloys, but was not important in the tungsten-osmium or tungsten-rhenium alloys. This may be attributable to the lower melting temperature of iridium. No conclusive evidence of surface texture dependence was observed. None of the materials tested exhibited a significant time dependence with respect to emissivity. Both the tungsten-osmium and tungsten-rhenium alloys exhibited emissivity values in the 0.32 to 0.54 range over the temperatures tested (1400 to 2600 K). The tungsten-iridium alloy yielded emissivity data in the 0.35 to 0.47 range (1400 to 2600 K). The niobium-ruthenium alloy emissivity data fell within 0.34 and 0.36 (1400 to 1950 K). The pure molybdenum and pure ruthenium experiments resulted in emissivity values from 0.35 to 0.45 and 0.35 to 0.39, respectively (1300 to 2300 K and 1400 to 2500 K). The data obtained in this work paralleled the data reported in the literature data where available.

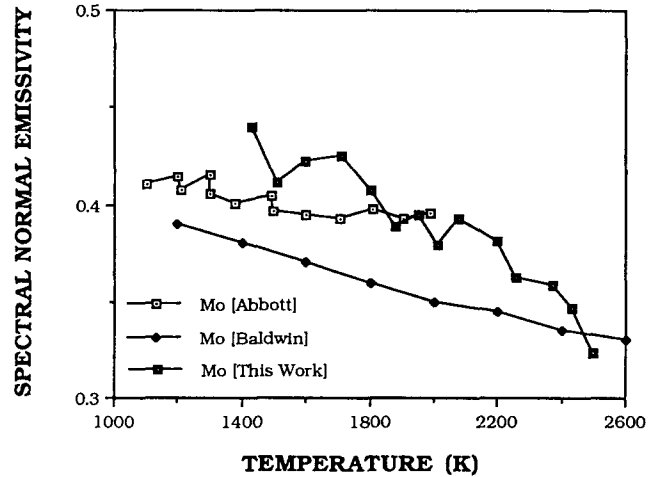


Fig. 8 Spectral normal emissivity of pure molybdenum at 0.65  $\mu\text{m}$  compared to experimental data.

## Acknowledgments

This work was funded by The Wright Research and Development Center, WPAPL, Ohio, under contract No. F33615-87-C-2769, Arizona State University. Also, the authors thank Dr. E.K. Storms (Los Alamos Scientific Laboratory) for his help in preparing the tungsten-osmium and tungsten-iridium alloys.

## References

1. D.P. DeWitt, "Comments on the Surface Characterization of Real Metals," NASA SP 55 (1964).
2. J.C. Richmond, "Importance of Surface Films," NASA SP 55 (1964).
3. H.H. Blau, Jr. and H.A. Jranicis, "Surface Properties of Metals," NASA SP 55 (1964).
4. R. Siegel and J.R. Howell, *Thermal Radiation Heat Transfer*, Hemisphere Publishing, New York (1981).
5. *Surface Texture (Surface Roughness, Waviness and Lay)*, ANSI/ASME B 46.1-1985, American Society of Mechanical Engineers (1985).
6. J.R. Branstetter and R.D. Schaal, "Thermal Emittance Behavior of Small Cavities Located on Refractory Metal Surfaces," NASA TM x-52147 (1965).
7. M. Planck, *Ann. Physik*, 4, 553 (1901).
8. P.H. Dike, in *High Temperature Technology*, I.E. Campbell, Ed., John Wiley & Sons, New York (1956).
9. E.M. Sherwood in *High Temperature Materials and Technology*, I.E. Campbell and E.M. Sherwood, Ed., John Wiley & Sons, (1967).
10. S.L. Isreal, T.D. Hawkins, and S.C. Hyman, NASA-CR-402, 1-46 (1966).
11. R.C. Good, Jr., Space Sciences Laboratory, General Electric Co., AFOSR-5096, 1-80 (1963).
12. D.M. Rosenbaum, E.M. Sherwood, I.E. Campbell, R.I. Jaffee, C.T. Sims, C.M. Craighead, E.N. Wyler, and F.C. Todd, BMI, Investigations of Rhenium, *Quart. Prog. Rept.*, No. 3, 1-40 (1953); AD 14174.
13. D.T.F. Marple, *J. Opt. Soc. Am.*, 46(7), 490-494 (1956).

14. R.W. Douglass and E.F. Adkins, *Trans. Metall. Soc. AIME*, 221(2), 248-249 (1961).
15. N.D. Konovalev, V.A. Kutznetsov, and B.M. Tsarev, *Sov. Phys. Tech. Phys.*, 14, 834 (1969).
16. N.O. Moraga and D.L. Jacobson, "High Temperature Emissivity Measurements of Tungsten-Rhenium Alloys," American Institute of Aeronautics and Astronautics 22nd Thermophysics Conference, Honolulu, June 8-10 (1987).
17. R.N. Wall, D.L. Jacobson, and D.R. Bosch, The High Temperature Electron Emission and Vaporization of Tungsten-Osmium Alloys, *Metall. Trans.*, accepted for publication.
18. G.K. Burgess and R.G. Waltenberg, *Natl. Bur. Std. Bull.*, 11, 591-605 (1915).
19. O.K. Husmann, *J. Appl. Phys.*, 37(13), 4662-4670 (1966).
20. R.N. Wall, D.L. Jacobson, and D.R. Bosch, *High Temp. Sci.*, 30, 95 (1991).
21. G.L. Abbott, WADD-TR-61-94 (Pt 3), 1-30 (1963).
22. R.W. Douglass and E.F. Adkins, *Trans. Metall. Soc. AIME*, 221(2), 248-249 (1961).
23. J. Baldwin, J.L. Shilts, and E.A. Coomes, in *Thermophysical Properties of High Temperature Solid Materials*, Vol I, Y.S. Touloukian, Ed., Macmillan, New York, 673 (1967).
24. G.L. Abbott, N.J. Alvares, and W.J. Parker, WADD-TR-61-94 (Pt 2), 1-31 (1962); AD 297865.